MATHEMATICAL BIOSCIENCES
AND ENGINEERING
Volume **10**, Number **5&6**, October & December **2013**

doi:10.3934/mbe.2013.10.1615

pp. **1615–1634**

OPTIMAL STRATEGIES OF SOCIAL DISTANCING AND VACCINATION AGAINST SEASONAL INFLUENZA

Eunha Shim

Department of Mathematics
University of Tulsa
Tulsa, OK 74104, USA

Abstract. Optimal control strategies for controlling seasonal influenza transmission in the US are of high interest, because of the significant epidemiological and economic burden of influenza. To evaluate optimal strategies of vaccination and social distancing, we used an age-structured dynamic model of seasonal influenza. We applied optimal control theory to identify the best way of reducing morbidity and mortality at a minimal cost. In combination with the Pontryagins maximum principle, we calculated time-dependent optimal policies of vaccination and social distancing to minimize the epidemiological and economic burden associated with seasonal influenza. We computed optimal age-specific intervention strategies and analyze them under various costs of interventions and disease transmissibility. Our results show that combined strategies have a stronger impact on the reduction of the final epidemic size. Our results also suggest that the optimal vaccination can be achieved by allocating most vaccines to preschool-age children (age under five) followed by young adults (age 20-39) and school age children (age 6-19). We find that the optimal vaccination rates for all age groups are highest at the beginning of the outbreak, requiring intense effort at the early phase of an epidemic. On the other hand, optimal social distancing of clinical cases tends to last the entire duration of an outbreak, and its intensity is relatively equal for all age groups. Furthermore, with higher transmissibility of the influenza virus (i.e. higher R0), the optimal control strategy needs to include more efforts to increase vaccination rates rather than efforts to encourage social distancing. Taken together, public health agencies need to consider both the transmissibility of the virus and ways to encourage early vaccination as well as voluntary social distancing of symptomatic cases in order to determine optimal intervention strategies against seasonal influenza.

1. **Introduction.** Seasonal influenza annually infects $10-20\%$ of the US population, resulting in about 200,000 hospitalizations and 36,000 deaths and an annual economic burden of $87.1 billion in the U.S. alone [14, 51]. The severe economic impacts of these recurring influenza epidemics include decreased workforce productivity, loss of life, and strained healthcare services [12, 35]. Worse, influenza is expected to become increasingly more widespread given current population growth and urbanization [53, 57].

The principal control strategy for controlling seasonal influenza transmission in the US is annual vaccination, recommended for all persons over the age of 6 months. To keep pace with the antigenic evolution of influenza, the influenza vaccine is updated annually and three strains identified as the ones most likely to be circulating

2010 *Mathematics Subject Classification.* Primary: 49J15, 62P10.
Key words and phrases. Optimal control theory, influenza, vaccination, social distancing.

among the population are selected for inclusion in the upcoming season's vaccine [14].

Children are considered to be the most responsible for the transmission of diseases such as influenza because of their high contact rate with their peers in school settings [5]. On the other hand, the influenza-related hospitalization and mortality burden is largely carried by people of ages over 65 years [31]. Indeed, the influenza-related hospitalization and mortality rates of elderly people are 20 and 100 times higher than those of people aged 5-49 [43, 44]. As a consequence, influenza vaccination is highly encouraged for the elderly, leading to relatively high vaccine coverage compared to that of other age groups. However, it has recently been shown that optimal influenza control in the entire population, including the elderly, can be achieved if vaccines are preferentially distributed to children and parents [30, 32, 51]. In fact, despite a rise in elder vaccination rates from 15% to 65% between 1985 and 2000, elderly influenza mortality rates remained largely unaffected [41], likely due to low vaccine efficacy among people aged 65 and older [17, 18].

Aside from vaccination, social distancing policy, often considered during a severe epidemic, dictates that infected individuals stay home from school or work [13, 23]. Social distancing interventions are known to reduce the overall illness attack rates and the consequential excess mortality attributed to influenza. Such interventions are also known to delay and reduce the peak attack rate, diminishing pressure on health services [23]. A recent study showed that social distancing measures such as school closures, isolation of symptomatic individuals, workplace non-attendance, and reduced community contact would prevent the development of influenza epidemics [23]. Another study arrived at a similar conclusion, finding that if social distancing measures are introduced early, they could notably mitigate the impact of future influenza pandemics [3]. Social distancing interventions such as reducing social and community contacts, and increasing home isolation are embedded within the pandemic influenza preparedness plans of most countries and are recommended by the WHO [20, 23]. For instance, during the early part of the 2009 H1N1 pandemic, the CDC (Centers for Disease Control and Prevention) recommended that those with influenza-like illness stay home from work for 7-10 days and an additional day after symptoms subsided [56]. However, social distancing controls can bear economic costs as well, as shown by a previous study on a cost analysis of control strategies for the 2009 H1N1 pandemic in Australia [19].

More comprehensive and combined strategies have been shown to be more successful than vaccination or social distancing alone [24]. The ability of mathematical modeling to predict the effectiveness of combined control strategies and positively influence public health policy is well established [16, 21, 24, 37, 52]. Based on approaches using optimal control theory, mathematical modeling studies have been carried out to define optimal strategies involving various interventions such as limited vaccine supply [26, 25], social distancing [29] and isolation [24]. Combined models of antiviral treatment and social distancing [16, 39], or vaccination and antiviral treatment [42] have also been proposed for influenza control and the application of optimal control theory. In addition, age-structured models of influenza transmission have indicated that optimal vaccine allocations differ markedly between age groups because both the risk of infection and its severity are dependent on age [7, 14, 21, 32, 36, 40, 45, 47].

Here, we propose an age-structured mathematical model of influenza transmission to assess time variations in age-specific vaccination and social distancing rates

Age group (i)	1	2	3	4	5	6
Ages (years)	0-5	6-12	13-19	20-39	40-59	60+
Initial population distribution (%)	8.14	9.32	9.34	26.90	27.20	19.10

TABLE 1. Population distribution in age groups

of infected individuals. Using optimal control theory, we determine the optimal strategies of age-specific vaccination and social distancing during seasonal influenza taking into consideration temporal dynamics of infection, hospitalization, and age-specific vaccine efficacy under different epidemiological scenarios. Specifically we examine the target age groups for vaccination, optimal timing of vaccination as well as social distancing of clinical cases that significantly reduce morbidity associated with seasonal influenza at a minimal cost.

2. **Method.** To model seasonal influenza transmission in the United States, we divide the population into the six age groups (0-5, 6-12, 13-19, 20-39, 40-59, and 60+). The numbers of people in each age group were set to values estimated for the U.S. 2012 population [54]. In our model, individuals in each age class are subdivided based on epidemiological status. Specifically, our model classifies individuals as susceptible (S_i), vaccinated (V_i), exposed (E_i), clinically ill and infectious (I_i), asymptomatic (A_i), hospitalized (J_i), recovered (R_i) and dead (D_i) for $i = 1, \ldots, 6$. The age groups are denoted by a subscript i.

It is assumed that susceptible individuals in age group i become infected at rate

$$\beta_i \sum_{j=1}^{m} \frac{\phi_{ij}(1-\rho_i)I_j}{N},$$

where ϕ_{ij} is the contact rate for infective individuals of age group j (I_j) with susceptible individuals of age group i (S_i) (see Appendix) [50]. In order to describe social distancing during a disease outbreak, we assume that infectious members in age group i decrease their rate of contact by a fraction $\rho_i(t)$ where $\rho_i(t) \in [0, 1]$. We define β_i as the probability of transmission per contact in age group i and calculate it based on the age-specific attack rate [35]. The total population size is given by $N(t) = \sum_{i=1}^{6} N_i(t) = \sum_{i=1}^{6}(S_i(t) + V_i(t) + E_i(t) + I_i(t) + A_i(t) + J_i(t) + R_i(t))$ where $N_i(t)$ the total number of individuals of age group i.

Susceptible individuals in age group i are assumed to be vaccinated at the rate of $\psi_i(t)$ where $\psi_i(t) \in [0, M]$. We assume that the vaccine provides partial protection, resulting in vaccinated individuals being less susceptible than unvaccinated ones. Specifically, the infection rate among vaccinated individuals in age group i is assumed to be reduced by vaccine efficacy, $\sigma_i(t)$, where $\sigma_i(t) \in [0, 1]$. Therefore, vaccinated individuals in age group i become infected at rate

$$(1-\sigma_i)\beta_i \sum_{j=1}^{m} \frac{\phi_{ij}(1-\rho_i)I_j}{N}.$$

Upon infection, individuals enter a latency period, $1/k$. Latently infected individuals proceed to become infectious, and a proportion, p, of infected individuals becomes symptomatic. We define b as relative infectiousness of asymptomatic cases compared to symptomatic ones. Both symptomatic and asymptomatic individuals

recover at the mean rate γ, while a proportion, $\alpha_i/(\gamma+\alpha_i)$, of symptomatic individuals in age group i are hospitalized. Hospitalized individuals either recover at the rate θ or die from influenza at the age-specific rate δ_i. Recovered individuals are assumed to be fully protected against further influenza infection for the remainder of the outbreak. The baseline values of epidemiological parameters are given in Table 2. The transmission dynamic model that incorporates the time-dependent (six age-specific) control functions, $\rho_i(t)$ and $\psi_i(t)$, is thus described by the following ordinary differential equations:

$$\begin{aligned}
S_i'(t) &= -\lambda_i S_i - \psi_i S_i,\\
V_i'(t) &= \psi_i S_i - (1-\sigma_i)\lambda_i V_i,\\
E_i'(t) &= \lambda_i\{S_i + (1-\sigma_i)V_i\} - kE_i,\\
I_i'(t) &= kpE_i - (\alpha_i+\gamma)I_i,\\
A_i'(t) &= k(1-p)E_i - \gamma A_i,\\
J_i'(t) &= \alpha_i I_i - (\theta_i+\delta_i)J_i,\\
R_i'(t) &= \gamma(A_i+I_i) + \theta_i J_i,\\
D_i'(t) &= \delta_i J_i,
\end{aligned} \tag{1}$$

where force of infection is given by $\lambda_i(t) = \beta_i \sum_{j=1}^{6} \frac{\phi_{ij}\{bA_j(t)+(1-\rho_j(t))I_j(t)\}}{N(t)}$. Initial conditions are defined as $S_i(0) = N_i(0) - \epsilon_i$, $V_i(0) = 0$, $E_i(0) = 0$, $I_i(0) = \epsilon_i$, $A_i(0) = 0$, $J_i(0) = 0$, $R_i(0) = 0$, and $D_i(0) = 0$ where $\epsilon_i > 0$ is small.

Note that the variable R_i and D_i appears only in the R_i' and D_i' differential equation, and the other variables do not depend on R_i or D_i. Thus, we consider the following system when we solve the optimality system, and determine $R_i(t)$ and $D_i(t)$ after solving for $S_i(t)$, $V_i(t)$, $E_i(t)$, $I_i(t)$ and $J_i(t)$.

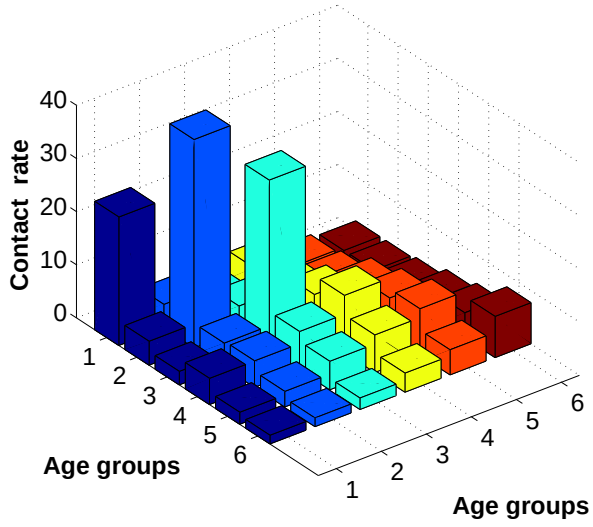

FIGURE 1. Age-dependent contact rate. The contact matrix ϕ_{ij} between age groups i and j per day is shown.

The age-structured mathematical model we will use is therefore

$$\begin{aligned} S_i'(t) &= -\lambda_i S_i - \psi_i S_i, \\ V_i'(t) &= \psi_i S_i - (1-\sigma_i)\lambda_i V_i, \\ E_i'(t) &= \lambda_i\{S_i + (1-\sigma_i)V_i\} - kE_i, \\ I_i'(t) &= kpE_i - (\alpha_i+\gamma)I_i, \\ A_i'(t) &= k(1-p)E_i - \gamma A_i, \\ J_i'(t) &= \alpha_i I_i - (\theta_i+\delta_i)J_i, \end{aligned} \tag{2}$$

where $\lambda_i = \beta_i \sum_{j=1}^{6} \frac{\phi_{ij}\{bA_j+(1-\rho_j)I_j\}}{N}$.

From our age-structured model, the expression for $\Re_0$ can be derived using the next-generation operator method. That is, $\Re_0 = r(FW^{-1})$, where $\Re_0$ is the spectral radius of the next generation matrix FW^{-1} [7, 8, 48]. In our model, the next generation matrix is given by

$$FW^{-1} = (M_{ij})_{i,j=1,\ldots,6}$$

where

$$M_{ij} = \beta_i \phi_{ij} \frac{N_k(0)}{N(0)} \left(\frac{p}{\gamma+\alpha_j} + \frac{(1-p)b}{\gamma} \right), \; i,j = 1,\ldots,6.$$

The objective functional to be minimized is

$$\mathcal{F}(\psi_i(t),\rho_i(t)) = \int_{t=0}^{T} \sum_{i=1}^{6} \{\chi_i I_i(t) + \Omega_i J_i(t) + B\rho_i^2(t) I_i(t) + C_i \psi_i^2(t) S_i(t)\} dt, \tag{3}$$

where the control effect is modeled by quadratic terms in $\psi(t)$ and $\rho(t)$. We assume that the control efforts are nonlinear (quadratic) to the objective functional. The control efforts are modeled by quadratic terms in order to incorporate the societal cost the associated with the implementation of control measures. Here, χ_i and ϖ_i are the costs associated with symptomatic infection and hospitalization per day for individuals in age group i, respectively. In addition, B is the relative opportunity cost associated with social distancing for infected individuals, and for simplicity, it is assumed to be invariant across age groups. We define C_i and $C_{V,i}$ as the relative cost of vaccination and the age-specific cost of vaccination, respectively, where $C_i = C_\kappa C_{V,i}$.

The age-dependent optimal strategies of vaccination and social distancing can be obtained by finding an optimal control functions, $\psi_i^*(t)$ and $\rho_i^*(t)$, such that

$$\mathcal{F}(\psi_i^*(t),\rho_i^*(t)) = \min_{\Theta} \mathcal{F}(\psi_i(t),\rho_i(t)) \tag{4}$$

subject to Model (2) where $\Theta = \{(\psi_i,\rho_i) \in L^1(0,T) | 0 \le \psi_i \le M, 0 \le \rho_i \le 1\}$. The control upper bound for vaccination, M, represents the maximum daily vaccination rate, which has been previously estimated at 0.02 [25, 55].

We use Pontryagins Maximum Principle to solve this optimal control problem and its optimality system [28]. Specifically, the necessary conditions that solutions to optimal problem Eq.(4) must satisfy are derived from Pontryagin's Maximum Principle. This principle converts our system (2)-(4) into the problem of minimizing

the Hamiltonian H given by

$$\begin{aligned}
H =& \sum_{i=1}^{6}\{\chi_i I_i(t) + \Omega_i J_i(t) + B\rho_i^2(t) I_i(t) + C_i\psi_i^2(t) S_i(t)\} \\
&+ \sum_{i=1}^{6} Q_{S_i}\left\{-S_i \sum_{j=1}^{6} \beta_i \phi_{ij}(bA_j + (1-\rho_j)I_j)/N - \psi_i S_i\right\} \\
&+ \sum_{i=1}^{6} Q_{V_i}\left\{-(1-\sigma_i)V_i \sum_{j=1}^{6} \beta_i \phi_{ij}(bA_j + (1-\rho_j)I_j)/N + \psi_i S_i\right\} \\
&+ \sum_{i=1}^{6} Q_{E_i}\left\{(S_i + (1-\sigma_i)V_i) \sum_{j=1}^{6} \beta_i \phi_{ij}(bA_j + (1-\rho_j)I_j)/N - kE_i\right\} \\
&+ \sum_{i=1}^{6} Q_{I_i}\{kpE_i - (\alpha_i + \gamma)I_i\} + \sum_{i=1}^{6} Q_{A_i}\{k(1-p)E_i - \gamma A_i\} \\
&+ \sum_{i=1}^{6} Q_{J_i}\{\alpha_i I_i - (\theta_i + \delta_i)J_i\}.
\end{aligned} \tag{5}$$

There exists a optimal control $(\psi^*(t), \rho^*(t))$ and corresponding solutions, S_i, V_i, E_i, I_i, A_i, and J_i $(i = 1, 2, \ldots, 6)$ that minimize $\mathcal{F}(\psi, \rho)$ over Ω [10]. The existence of optimal controls follows from Corollary 4.1 of [10] and is guaranteed by standard results in control theory. That is, the convexity of integrand $\mathcal{F}$ with respect to (ψ, ρ) is satisfied, and the state system satisfies the *Lipschitz* property with respect to state variables. Applying Pontryagin's Maximum Principle, we obtain the following adjoint system [38]:

$$\frac{dQ_{S_i}}{dt} = -\frac{\partial H}{\partial S_i}, \ \frac{dQ_{V_i}}{dt} = -\frac{\partial H}{\partial V_i}, \ \frac{dQ_{E_i}}{dt} = -\frac{\partial H}{\partial E_i},$$

$$\frac{dQ_{I_i}}{dt} = -\frac{\partial H}{\partial I_i}, \ \frac{dQ_{A_i}}{dt} = -\frac{\partial H}{\partial A_i}, \ \frac{dQ_{J_i}}{dt} = -\frac{\partial H}{\partial J_i},$$

evaluated at the optimal controls and corresponding states $(i = 1, 2, \ldots, 6)$. The equations above reduce to

$$\begin{aligned}
\frac{dQ_{S_i}}{dt} =& (Q_{S_i} - Q_{V_i})\psi_i - C_i\psi_i^2(t) + (Q_{S_i} - Q_{E_i}) \sum_{j=1}^{6} \beta_i \phi_{ij}\{(1-\rho_j)I_j + bA_j\}/N, \\
\frac{dQ_{V_i}}{dt} =& (Q_{V_i} - Q_{E_i})(1-\sigma_i) \sum_{j=1}^{6} \beta_i \phi_{ij}\{(1-\rho_j)I_j + bA_j\}, \\
\frac{dQ_{E_i}}{dt} =& k\{Q_{E_i} - pQ_{I_i} - (1-p)Q_{A_i}\}, \\
\frac{dQ_{I_i}}{dt} =& -\chi_i - B\rho_i^2(t) + (\alpha_i + \gamma)Q_{I_i} - \alpha_i Q_{J_i} \\
&+ (1-\rho_i) \sum_{j=1}^{6} \frac{\beta_i \phi_{ji}}{N}\{S_j(Q_{S_j} - Q_{E_j}) + (1-\sigma_j)V_j(Q_{V_j} - Q_{E_j})\},
\end{aligned} \tag{6}$$

$$\frac{dQ_{A_i}}{dt} = \gamma Q_{A_i} + \sum_{j=1}^{6} \frac{\beta_i \phi_{ji} b}{N} \{S_j(Q_{S_j} - Q_{E_j}) + (1-\sigma_j)V_j(Q_{V_j} - Q_{E_j})\},$$

$$\frac{dQ_{J_i}}{dt} = -\Omega_i + (\theta_i + \delta_i)Q_{J_i}.$$

The transversality conditions are

$$Q_{S_i}(T) = Q_{V_i}(T) = Q_{E_i}(T) = Q_{I_i}(T) = Q_{A_i}(T) = Q_{J_i}(T) = 0\,(i = 1, 2, \ldots, 6).$$

The Hamiltonian H is minimized with respect to the controls, giving the following optimality conditions:

$$\frac{\partial H}{\partial \psi_i} = 0,\ \frac{\partial H}{\partial \rho_i} = 0\,(i = 1, 2, \ldots, 6)$$

at $\psi_i(t) = \psi_i^*(t)$ and $\rho_i(t) = \rho_i^*(t)$. Solving for ψ and ρ subject to the constraints, we obtain:

$$\psi_i^*(t) = \min\left\{\max\left\{0, \frac{(Q_{S_i} - Q_{V_i})}{2C_i}\right\}, M\right\},$$

$$\rho_i^*(t) = \min\left\{\max\left\{0, \rho_i^{\#}\right\}, 1\right\}.$$

where

$$\rho_i^{\#} = \frac{1}{2B_i} \sum_{j=1}^{6} \frac{\beta_i \phi_{ji}}{N} \{S_j(Q_{E_j} - Q_{S_j}) + (1-\sigma_j)V_j(Q_{E_j} - Q_{V_j})\}.$$

3. **Numerical results.** Here, we analyzed numerically an optimal control strategy applied to our model of influenza transmission, and show representative numerical simulations to illustrate the results of applying optimal controls to our model under two scenarios. The first scenario considers vaccination without social distancing. In the second scenario, both social distancing of clinical cases and vaccination are implemented simultaneously.

Numerical solutions to the optimality system, model 2 and adjoint Eq. 6, were carried out using the forward-backward scheme [28]. Starting with an initial guess for the optimal controls, $\psi_i(t)$ and $\rho_i(t)$, the state variables were solved forward in time from model 2 using the forward Euler method. Next, state variables and the transversality conditions were used to solve the adjoint Eq. 6 backward in time. The controls, $\psi_i(t)$ and $\rho_i(t)$, were updated, and the error between their old and updated values was calculated. This iterative process terminates when the error is less than a pre-assigned value, 0.00001. The final values of $\psi_i(t)$ and $\rho_i(t)$ via the above method were used as our numerical approximations to the optimal control solutions. Unless otherwise specified, we used the values in Table 2 as a baseline parameter set for simulations. Results of the sensitivity analyses on key model parameters such as a basic reproductive ratio and weight constants were also determined.

Parameter	Description	Value	References
$\Re_0$	Basic reproductive ratio	1.85	[33, 46]
β_i	Probability of transmission per contact	0.05 for $i = 1$ 0.02 for $i = 2, 3, 4, 5$ 0.03 for $i = 6$	[35]
σ_i	Age-specific protective efficacy of vaccination	0.6 for $i = 6$; 0.8 otherwise	[11]
b	Relative infectiousness of asymptomatic cases compared to symptomatic cases	0.142	[34]
p	Proportion of infected individuals who become symptomatic	0.33	[40]
k	Rate of progression from latent to infectious class (days^{-1})	1/1.2	[11]
γ	Recovery rate for infectious class (days^{-1})	1/4	[11]
α_i	Age-specific diagnostic rate (days^{-1})	0.001 for $i = 1, 2, 3$ 0.002 for $i = 4$ 0.003 for $i = 5$ 0.007 for $i = 6$	[6]
θ	Recovery rate for hospitalized individuals (days^{-1})	0.34	[24]
δ_i	Age-specific mortality rate (days^{-1})	0.001 for $i = 1$ 0.007 for $i = 2, 3, 4$ 0.016 for $i = 5$ 0.065 for $i = 6$	[6]
T	The simulated duration (days)	150	
M	The upper bound of vaccination rates (days^{-1})	0.02	[25]
B	Weight constant on social-distancing control	500	Author's assumption
C_κ	Weight constant on vaccination	50	Author's assumption
$C_{V,i}$	Cost of vaccine and vaccine administration	\$50 for $i = 1$ \$45 for $i = 2$ \$41 for $i = 3$ \$32 for $i = 4, 5, 6$	[6]

TABLE 2. Definition of parameters and baseline values used in numerical simulations.

3.1. **Optimal vaccination strategy.** To understand the effects of optimal vaccination strategies on the dynamics of seasonal influenza, we first simulated our model (2) without any control measure, i.e. $\psi_i(t) = 0$ and $\rho_i(t) = 0$. In the absence of intervention, the cumulative proportion of clinical cases is estimated at 23% (Fig 2(c)). Specifically, 31% of pre-school children, $23 - 24$% of school-aged children and adults, and 20% of the elderly (aged 65+) are estimated to be clinically infected with seasonal influenza in the absence of any control measure.

Next, in order to highlight the exclusive use of vaccination as a control measure, we computed the optimal strategy for seasonal influenza when vaccination was the only control, i.e. $\rho_i(t) = 0$ (Fig 2). Our results illustrate the optimal control functions computed as a function of time using baseline parameters in Table 2 (Fig 2(a)). The corresponding cumulative vaccine coverage levels and daily incidence of the symptomatic class in the presence and absence of optimal vaccination are also computed (Figs 2(b) and 2(c)). The optimal vaccination rates for all age groups were found to be the highest at the beginning of the outbreak, requiring intense effort for the first 30 days for the youngest age group (Fig 2(a)). The optimal rate of vaccination decreases gradually for all age groups over time. Such pattern of optimal vaccination is consistent with previous studies ([2, 39]) in that the optimal control solution always appears to be one in which maximum effort is required at the beginning of the outbreak. Our results indicate that the optimal vaccine coverage

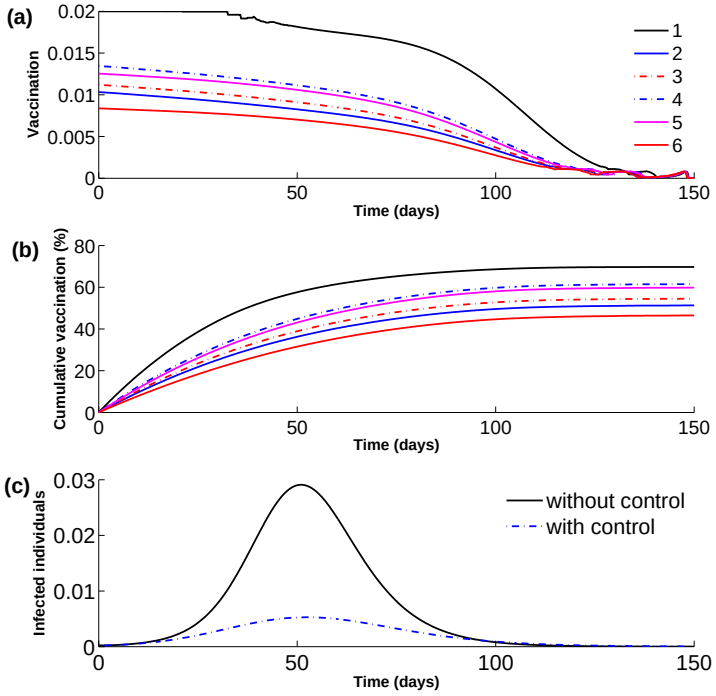

FIGURE 2. Optimal vaccination rate, $\psi_i(t)$, as a function of time in the absence of social distancing policy. (a) The age-specific optimal vaccination rates are calculated. Figure legends indicate age groups (Table 1). (b) Age-specific levels of cumulative vaccination when optimal vaccination strategy is applied. (c) The corresponding daily incidence of symptomatic infections, $\Sigma_{i=1}^{6} I_i(t)$, under no controls with those generated with optimal vaccination control are compared.

level is highest in preschool-age children under five years of age, followed by younger and older adults (age $20-39$ and $40-59$, respectively), while the elderly (age 65 and older) achieve the lowest vaccine coverage level. During the entire duration of an influenza epidemic, the optimal vaccination rate for the preschool-age children is found to maintain the highest level of vaccination rate among all age groups, achieving 70% of vaccine coverage eventually. This is because the susceptibility among the preschool-age children (β_1) is highest, and the size of this age group is relatively small. Vaccinating younger and older adults also provides indirect protection of preschool-age children due to their relatively high contact rates.

In our model, a significant reduction in the size of the outbreak is observed when vaccination is the sole control measure. The dynamics of a natural single outbreak are significantly affected by introducing optimal vaccination (Fig 2(c)). In fact, our results indicate that vaccination reduces the total morbidity by over 60% for all age groups when the optimal vaccination strategy is employed (Fig 4).

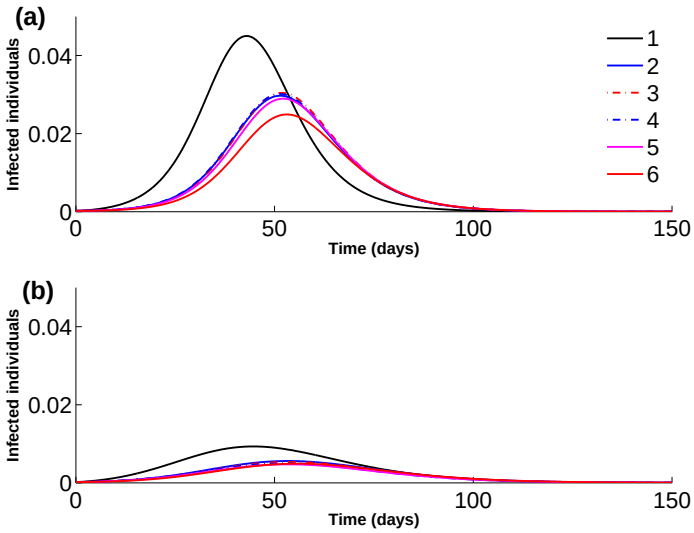

FIGURE 3. Dynamics of the symptomatic classes ($I_i(t)$) in age groups. We compare a baseline situation where no vaccine is used (a) with results implementing optimal vaccination strategies (b). Social distancing measure is not implemented in both cases ($\rho_i(t) = 0$).

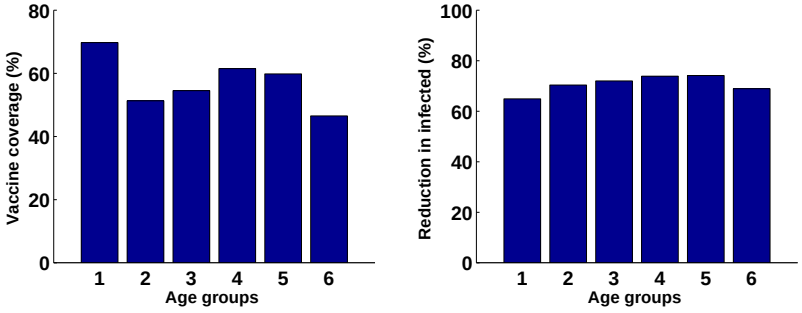

FIGURE 4. Optimal vaccine coverage and the resulting reduction in influenza incidence. (a) Age-specific optimal vaccine coverage levels are illustrated. (b) The percent age-specific reductions in infected (symptomatic) classes are shown relative to the situation where no intervention is applied).

The optimal vaccination strategies are found to be highly dependent on the costs of vaccination (Figs 5 and 6). In general, as the cost of vaccination increases, we observed dramatic decrease in the level of the optimal vaccination rate, $\psi_i(t)$, although the optimal control function and the resulting influenza outbreak are qualitatively similar to the baseline case with $C_\kappa = 50$. For illustration purpose, we selected

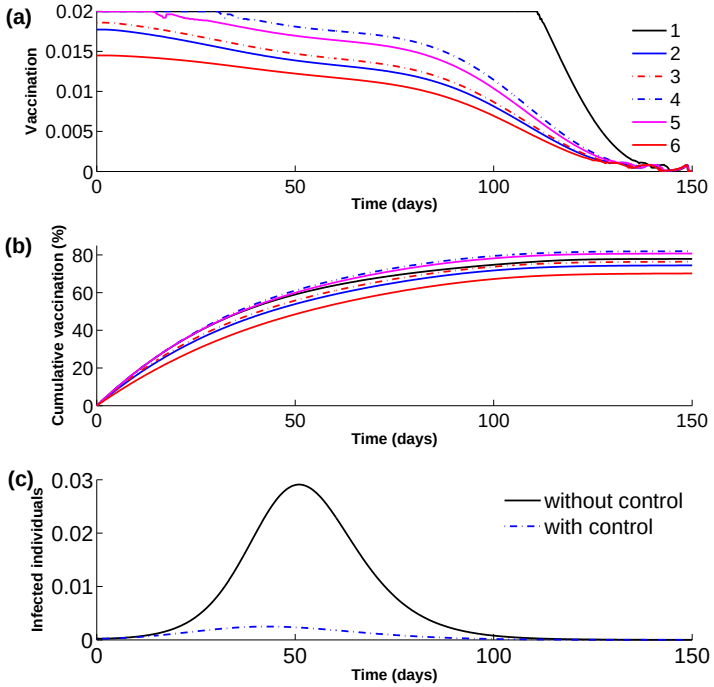

FIGURE 5. The impact of decreased weight constants on age-specific vaccination rates. (a) Using the weight constant, $C_{\kappa,i} = 10$, results in the lower vaccination rates for all age groups. (b) The corresponding cumulative vaccine coverage levels in age groups are presented. (b) The corresponding curves illustrating the number of infections at time t ($I(t)$) with optimal vaccination and no control are presented.

simulations where the cost of implementing vaccination is either 20% of the baseline value (Fig 5) or is increased two-fold over the baseline value ($C_\kappa = 50$) (Figs 6). In general, higher relative vaccination costs result in an increase in the total number of influenza cases. In the case where the weight constant for vaccination (C_κ) is reduced to 10, we observed a significant increase in the level of optimal vaccine coverage for all age groups, achieving 78% of vaccine coverage on average for the population (Fig 5). This overall vaccine coverage is reduced to 41% when the weight constant for vaccination (C_κ) is increased to 100. The percent reduction in the number of symptomatic cases of this single control strategy is 88% if C_κ equals 10 and decreases dramatically to 50% if vaccination is relatively costly ($C_\kappa = 100$) (Figs 5(c) and 6(c)).

3.2. **Optimal combined strategy of vaccination and social distancing.** To present the optimal strategy when social distancing and vaccination control measures are implemented simultaneously, the numerical solutions of optimal controls, $\psi_i(t)$ and $\rho_i(t)$, are computed (Fig 7). The optimal control strategies of both social

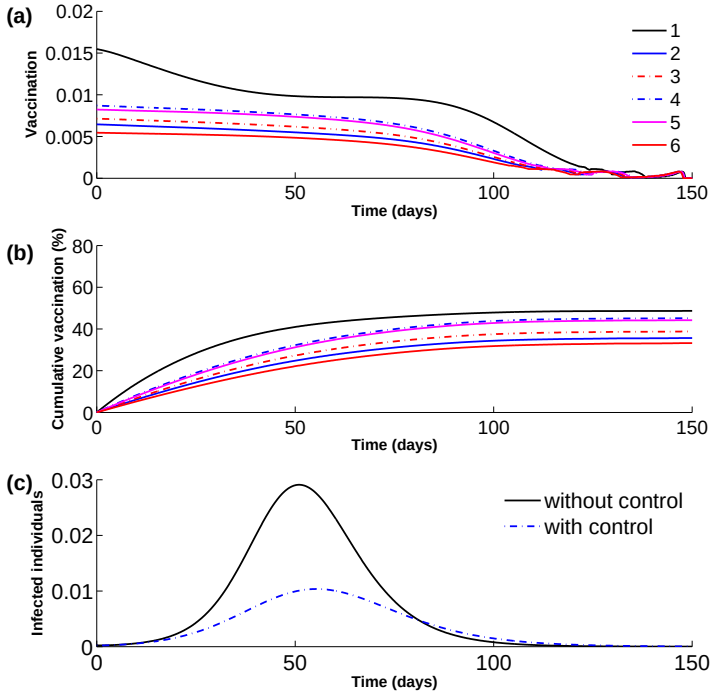

FIGURE 6. The impact of increased weight constants on age-specific vaccination rates. (a) Using the weight constant, $C_{\kappa,i} = 100$, results in the higher vaccination rates for all age groups. (b) The corresponding cumulative vaccine coverage levels in age groups are presented. (b) The corresponding curves illustrating the number of infections at time t ($I(t)$) with optimal vaccination and no control are presented.

distancing and vaccination require maximum effort, i.e. upper bound of $\psi_i(t)$ and $\rho_i(t)$, at the beginning of the outbreak. Specifically, symptomatic individuals of all ages are expected to do social distancing with a probability of $\rho_{max}(t)$ for more than 60 days. Social distancing is more costly than vaccination by our modeling assumption and yet, according to our results, most of the intervention effort should be placed in social distancing of infected individuals throughout the outbreak in order to achieve optimal controls at minimal cost (Fig 7(d)). Taken together, our results showed that in order to minimize the epidemiological burden of seasonal influenza at minimal cost, social distancing efforts for symptomatic individuals of all ages must be kept near the maximum through the entire duration of an influenza epidemic, while vaccination of preschool-age children under five years of age needs to be prioritized (Fig 7). Throughout the epidemic, our results indicate that optimal vaccination rate for this youngest age group is significantly higher than for other age groups, followed by adults (age $20-59$), school-age children (ages $6-19$) and the elderly (ages 65+).

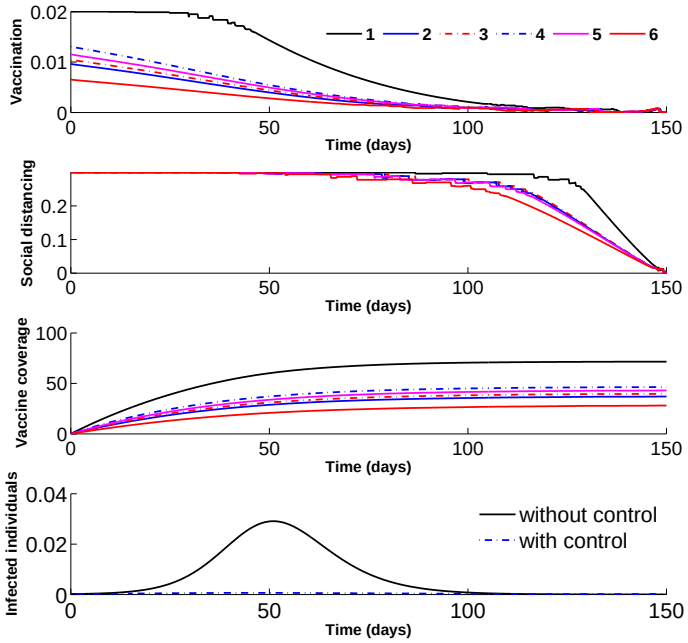

FIGURE 7. Optimal control strategies of vaccination rate and social distancing ($\psi_i(t)$ and $\rho_i(t)$, respectively). (a) The age-specific optimal vaccination rates are calculated. Figure legends indicate age groups (Table 1). (b) The age-specific optimal strategies of social distancing are calculated. (c) Age-specific levels of cumulative vaccination when optimal vaccination strategy is applied. (d) The corresponding daily incidence of symptomatic infections, $\Sigma_{i=1}^{6} I_i(t)$, under no controls with those generated with optimal vaccination control are compared.

The dual controls of vaccination and social distancing of symptomatic cases are so effective that they nearly eradicate the disease (Fig 7(d) and Fig 8(d)). In fact, the implementation of the optimal controls (social distancing and vaccination) immediately suppresses the outbreak (Fig 7(d)), reducing the total number of influenza cases by over 90% for all age groups (Fig 8).

Social distancing, in reality, is hard to be in practice completely, so we assume the maximum level (ρ_{max}) of adherence of social distancing in our model, when defining optimal strategies of social distancing which minimize economic burden associated with influenza epidemic and control efforts. Increasing this maximum adherence of social distancing (ρ_{max}) to 0.5 leads to an optimal control policy that puts more effort into social distancing of clinical cases than with baseline value of ρ_{max}, 0.3 (Fig 9). The higher the maximum adherence level to social distancing becomes, the more emphasis should be placed on social distancing in order to achieve optimized control efforts. In fact, it was shown that a reduction of 98% in the final epidemic size can be achieved when ρ_{max} is increased to 0.5 (Fig 9(d)). Such

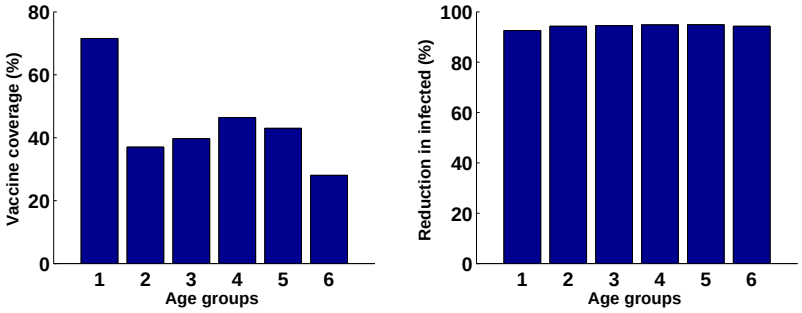

FIGURE 8. Optimal vaccine coverage and the resulting reduction in influenza incidence. (a) Age-specific optimal vaccine coverage levels are illustrated when both optimal strategies of vaccination and social distancing are used. (b) The percent age-specific reductions in infected (symptomatic) classes are shown relative to the situation where no intervention is applied.

epidemiological impact is achieved even if optimal vaccination levels are relatively low. Specifically, when the maximum adherence level to social distancing is 0.3, the optimal cumulative vaccination levels range from 15% among the elderly (age 65+) to 57% among preschool-age children, leading to an average of 25% vaccine coverage levels overall (Fig 9(c)).

We also analyzed the effects of a basic reproductive ratio of seasonal influenza on the optimal control strategies of vaccination and social distancing. The reproductive ratio for seasonal influenza is estimated to be $\Re_0 = 1.6 - 3.0$ [46]. Our results indicate that with a higher basic reproductive ratio ($\Re_0 = 2.5$), the optimal rate of vaccination (and thus optimal vaccine coverage levels) increases for all age groups (Fig 10). Furthermore, the duration for which we should implement vaccination for the youngest age group at maximum effort at the beginning of the outbreak increases. With $\Re_0 = 2.5$, 29% of the population would be clinically infected without control measures, resulting in a risk of infection in the range of 26% to 33% in the youngest age group (age $0 - 5$) and among the elderly (age 65+), respectively. When optimal dual strategies are applied (vaccination and social distancing of clinical cases), the highest optimal vaccine coverage, 71%, is achieved among pre-school children (aged $0 - 5$) and adults (aged $20 - 59$). On average, the overall optimal vaccination coverage across age groups is estimated to be 67%, reducing symptomatic infections by 82%. On the other hand, as $\Re_0$ increases, the duration for which we should implement social distancing at maximum effort at the beginning of the outbreak decreases. For the case where $\Re_0 = 2.5$, the optimal control function, $\rho_i(t)$ is at a maximum for just over 40 days, compared to more than 60 days when $\Re_0 = 1.85$. In addition, optimal social distancing for individuals of age 6 or greater is reduced once the peak of an outbreak appears.

4. **Discussion.** To evaluate optimal strategies of vaccination and social distancing against seasonal influenza, we used a mathematical model of the transmission dynamics of seasonal influenza that accounted for age heterogeneity in disease transmissibility, in addition to age-specific rates of infection, hospitalization, and

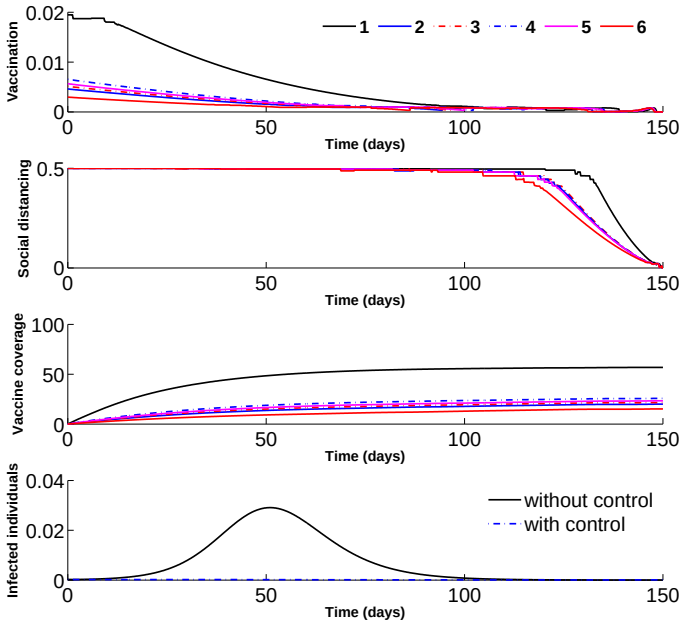

FIGURE 9. The impact of the upper bound for the probability of social distancing (ρ_{max}) on the optimal control strategies, $\psi_i(t)$ and $\rho_i(t)$. In this simulations, ρ_{max} was increased to 0.5. (a) The age-specific optimal vaccination rates are calculated. Figure legends indicate age groups (Table 1). (b) The age-specific optimal strategies of social distancing are calculated. (c) Age-specific levels of cumulative vaccination when optimal vaccination strategy is applied. (d) The corresponding daily incidence of symptomatic infections, $\Sigma_{i=1}^{6} I_i(t)$, under no controls with those generated with optimal vaccination control are compared.

death. Our mathematical framework incorporated time-dependent social distancing of symptomatic cases and vaccination rates into the optimal control framework. We computed optimal vaccination policies and analyzed them in the absence and presence of social distancing. Earlier implementation of vaccination has always the greatest effect on the final size of infected individuals. Furthermore, dual strategies are more efficient at reducing the final epidemic size than a single vaccination policy. The simulation of the model with two controls (dual policy) showed that increasing the basic reproductive ratio would result in higher optimal vaccination rates, but lower levels of social distancing.

Our results further indicate that the optimal vaccination coverage differs between age groups both in the absence and presence of social distancing. Specifically, the highest vaccination rate is allocated to 0-5 year olds, followed by adults (age 20-59), school-age children (age 6-19), and the elderly (age 65+), both in the absence and presence of social distancing. This pattern was consistent for a higher basic

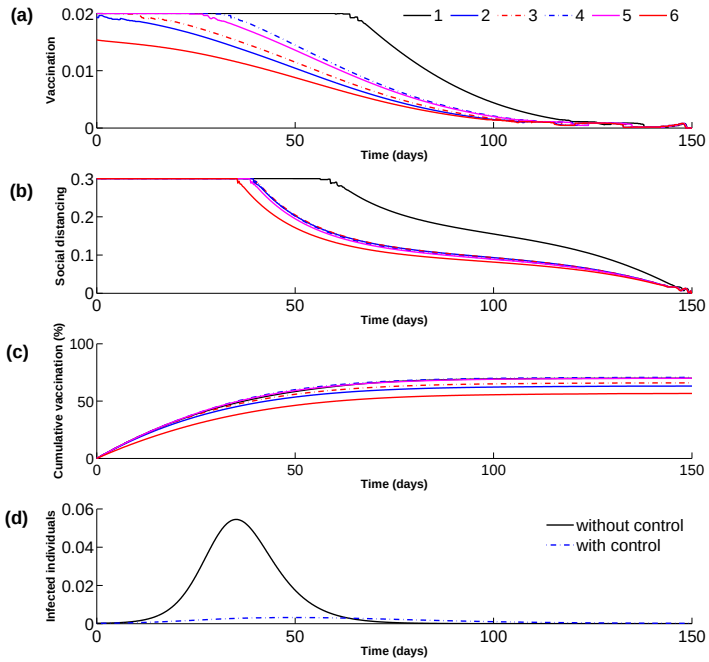

FIGURE 10. The impact of a basic reproductive ratio ($\Re_0$) on the optimal control strategies, $\psi_i(t)$ and $\rho_i(t)$. In this simulations, $\Re_0$ was increased to 2.5. (a) The age-specific optimal vaccination rates are calculated. Figure legends indicate age groups (Table 1). (b) The age-specific optimal strategies of social distancing are calculated.

reproductive ratio (i.e. higher transmissibility of influenza virus) and for a higher cost of vaccination. Our analysis confirmed that relatively high contact rates within the pre-school age group (0-5 yr) and their smaller population size (thus relatively lower cost for vaccinating this age group than others) resulted in the highest optimal vaccination rate, both in the absence and presence of social distancing. Overall, the optimal vaccination strategy provided relatively high reductions of over 63% for all age groups in the number of symptomatic cases with our baseline parameters. Our findings also indicate that the duration of the intensive vaccination period for optimal policy depends on the transmissibility of the virus and on vaccination cost. Specifically, the higher the transmissibility of the virus is, the longer the intensive vaccination efforts need to be implemented. On the other hand, higher cost of vaccine implementation tends to shorten the duration of optimal vaccination.

Our results suggest that annual influenza vaccination of preschool-age children should be strongly encouraged. Infection rates among children are relatively high during typical influenza seasons, averaging $25\% - 43\%$, and their epidemic peak is earlier than for other age groups [51]. In addition, younger children are most responsible for the transmission of influenza, especially within households [51]. Thus,

routine childhood vaccination would prevent a substantial number of influenza cases by directly protecting the children. Routine vaccination would also generate external benefits by reducing disease transmission among the rest of the population.

Contact reduction measures among clinical cases can also be an effective part of mitigation strategies. The advantage of such measures over vaccination is that these measures do not need to be limited, i.e. they can be continued for a sufficiently long period of time. As shown for other disease outbreaks such as SARS and pandemic influenza ([9, 49]), self-isolation and social distancing measures can be highly effective, reducing the transmission of disease significantly. Therefore, control strategies of seasonal influenza should include efforts to encourage social distancing as well as early vaccination.

Appendix. The contact matrix ϕ_{ij} represents the mixing rate between individuals of age group i and j per day ([25, 50]), which is given by

$$\phi_{ij} = \begin{bmatrix} 24.16 & 4.50 & 2.54 & 4.93 & 2.26 & 1.64 \\ 4.50 & 39.22 & 4.62 & 4.98 & 2.94 & 1.64 \\ 2.54 & 4.62 & 32.04 & 7.25 & 5.36 & 2.14 \\ 4.93 & 4.98 & 7.25 & 10.81 & 7.06 & 3.58 \\ 2.26 & 2.94 & 5.36 & 7.06 & 8.75 & 4.71 \\ 1.64 & 1.64 & 2.14 & 3.58 & 4.71 & 7.75 \end{bmatrix}.$$

Acknowledgments. Research reported in this publication was supported by the National Institute of General Medical Science of the National Institutes of Health under award number U54GM088491.

REFERENCES

[1] R. M. Anderson and R. M. May, "Infectious Diseases of Humans," Oxford University Press, Oxford, 1991.

[2] H. Behnke, *Optimal control of deterministic epidemics*, Optimal Control Application Methods, **21** (2000), 269–285.

[3] K. J. Bolton, J. M. McCaw, R. Moss, R. S. Morris, S. Wang, A. Burma, B. Darma, D. Narangerel, P. Nymadawa and J. McVernon, *Likely effectiveness of pharmaceutical and non-pharmaceutical interventions for mitigating influenza virus transmission in Mongolia*, Bull World Health Organization, **90** (2012), 264–271.

[4] F. Brauer and C. Castillo-Chavez, "Mathematical Models in Population Biology and Epidemiology," 2^{nd} edition, Texts in Applied Mathematics, **40**, Springer, New York, 2012.

[5] J. S. Brownstein, K. P. Kleinman and K. D. Mandl, *Identifying pediatric age groups for influenza vaccination using a real-time regional surveillance system*, Am. J. Epidemiol, **162** (2005), 1–8.

[6] K. M. Clements, J. Chancellor, K. Nichol, K. DeLong and D. Thompson, *Cost-effectiveness of a recommendation of universal mass vaccination for seasonal influenza in the United States*, Value Health, **14** (2011), 800–811.

[7] G. Chowell, C. Viboud, X. Wang, S. M. Bertozzi and M. A. Miller, *Adaptive vaccination strategies to mitigate pandemic influenza: Mexico as a case study*, PLoS One, **4** (2009), e8164.

[8] O. Diekmann and J. Heesterbeek, "Mathematical Epidmeiology of Infectious Diseases: Model Building, Analysis and Interpretation," Wiley Series in Mathematical and Computational Biology, John Wiley & Sons, Ltd., Chichester, 2000.

[9] H. P. Duerr, S. O. Brockmann, I. Piechotowski, M. Schwehm and M. Eichner, *Influenza pandemic intervention planning using InfluSim: Pharmaceutical and non-pharmaceutical interventions*, BMC Infect. Dis., **7** (2007).

[10] W. H. Fleming and R. W. Rishel, "Deterministic and Stochastic Optimal Control," Applications of Mathematics, No. 1, Springer-Verlag, Berlin-New York, 1975.

[11] A. P. Galvani, T. C. Reluga and G. B. Chapman, *Long-standing influenza vaccination policy is in accord with individual self-interest but not with the utilitarian optimum*, Proc. Natl. Acad. Sci. USA, **104** (2007), 5692–5697.
[12] R. Gasparini, D. Amicizia, P. L. Lai and D. Panatto, *Clinical and socioeconomic impact of seasonal and pandemic influenza in adults and the elderly*, Hum. Vaccin. Immunother., **8** (2012), 21–28.
[13] R. J. Glass, L. M. Glass, W. E. Beyeler and H. J. Min, *Targeted social distancing design for pandemic influenza*, Emerg. Infect. Dis., **12** (2006), 1671–1681.
[14] J. Glasser, Z. Feng, A. Moylan, S. Del Valle and C. Castillo-Chavez, *Mixing in age-structured population models of infectious diseases*, Math. Biosci., **235** (2012), 1–7.
[15] J. Glasser, D. Taneri, Z. Feng, J. H. Chuang, P. Tll, W. Thompson, M. McCauley and J. Alexander, *Evaluation of targeted influenza vaccination strategies via population modeling*, PLoS One, **5** (2010), e12777.
[16] P. A. Gonzalez-Parra, S. Lee, L. Velazquez and C. Castillo-Chavez, *A note on the use of optimal control on a discrete time model of influenza dynamics*, Math. Biosci. Eng., **8** (2011), 183–197.
[17] T. M. Govaert, C. T. Thijs, N. Masurel, M. J. Sprenger, G. J. Dinant and J. A. Knottnerus, *The efficacy of influenza vaccination in elderly individuals. A randomized double-blind placebo-controlled trial*, JAMA, **272** (1994), 1661–1665.
[18] P. A. Gross, A. W. Hermogenes, H. S. Sacks, J. Lau and R. A. Levandowski, *The efficacy of influenza vaccine in elderly persons. A meta-analysis and review of the literature*, Ann. Intern. Med., **123** (1995), 518–527.
[19] N. Halder, J. K. Kelso and G. J. Milne, *Cost-effective strategies for mitigating a future influenza pandemic with H1N1 2009 characteristics*, PLoS One, **6** (2011), e22087.
[20] J. S. Horvath, M. McKinnon and L. Roberts, *The Australian response: Pandemic influenza preparedness*, Med. J. Aust., **185** (2006), S35–8.
[21] M. J. Keeling and L. Danon, *Mathematical modelling of infectious diseases*, Br. Med. Bull., **92** (2009), 33–42.
[22] M. J. Keeling and P. J. White, *Targeting vaccination against novel infections: Risk, age and spatial structure for pandemic influenza in Great Britain*, J. R. Soc. Interface, **8** (2011), 661–670.
[23] J. K. Kelso, G. J. Milne and H. Kelly, *Simulation suggests that rapid activation of social distancing can arrest epidemic development due to a novel strain of influenza*, BMC Public Health, **9** (2009).
[24] S. Lee, G. Chowell and C. Castillo-Chavez, *Optimal control for pandemic influenza: The role of limited antiviral treatment and isolation*, J. Theor. Biol., **265** (2010), 136–150.
[25] S. Lee, M. Golinski and G. Chowell, *Modeling optimal age-specific vaccination strategies against pandemic influenza*, Bull. Math. Biol., **74** (2012), 958–980.
[26] S. Lee, R. Morales and C. Castillo-Chavez, *A note on the use of influenza vaccination strategies when supply is limited*, Math. Biosci. Eng., **8** (2011), 171–182.
[27] V. J. Lee, D. C. Lye and A. Wilder-Smith, *Combination strategies for pandemic influenza response - a systematic review of mathematical modeling studies*, BMC Med., **7** (2009).
[28] S. Lenhart and J. T. Workman, "Optimal Control Applied to Biological Models," Chapman & Hall/CRC Mathematical and Computational Biology Series, Chapman & Hall/CRC, Boca Raton, FL, 2007.
[29] F. Lin, K. Muthuraman and M. Lawley, *An optimal control theory approach to non-pharmaceutical interventions*, BMC Infect. Dis., **10** (2010).
[30] I. M. Longini, Jr. and M. E. Halloran, *Strategy for distribution of influenza vaccine to high-risk groups and children*, Am. J. Epidemiol., **161** (2005), 303–306.
[31] A. M. McBean and P. L. Hebert, *New estimates of influenza-related pneumonia and influenza hospitalizations among the elderly*, Int. J. Infect. Dis., **8** (2004), 227–235.
[32] J. Medlock and A. P. Galvani, *Optimizing influenza vaccine distribution*, Science, **325** (2009), 1705–1708.
[33] G. N. Mercer, S. I. Barry and H. Kelly, *Modelling the effect of seasonal influenza vaccination on the risk of pandemic influenza infection*, BMC Public Health, **11** (2011), S11.
[34] S. M. Moghadas, C. S. Bowman, G. Rst and J. Wu, *Population-wide emergence of antiviral resistance during pandemic influenza*, PLoS One, **3** (2008), e1839.

[35] N. A. Molinari, I. R. Ortega-Sanchez, M. L. Messonnier, W. W. Thompson, P. M. Wortley, E. Weintraub and C. B. Bridges, *The annual impact of seasonal influenza in the US: Measuring disease burden and costs*, Vaccine, **25** (2007), 5086–5096.

[36] S. D. Mylius, T. J. Hagenaars, A. K. Lugnr and J. Wallinga, *Optimal allocation of pandemic influenza vaccine depends on age, risk and timing*, Vaccine, **26** (2008), 3742–3749.

[37] H. Nishiura, C. Castillo-Chavez, M. Safan and G. Chowell, *Transmission potential of the new influenza A(H1N1) virus and its age-specificity in Japan*, Euro. Surveill., **14** (2009), 19227.

[38] L. S. Pontryagin, V. G. Boltyanskii, R. V. Gamkrelidze and E. F. Mishchenko, "The Mathematical Theory of Optimal Processes," Interscience Publishers John Wiley & Sons, Inc., New York-London, 1962.

[39] O. Prosper, O. Saucedo, D. Thompson, G. Torres-Garcia, X. Wang and C. Castillo-Chavez, *Modeling control strategies for concurrent epidemics of seasonal and pandemic H1N1 influenza*, Math. Biosci. Eng., **8** (2011), 141–170.

[40] E. Shim, L. A. Meyers and A. P. Galvani, *Optimal H1N1 vaccination strategies based on self-interest versus group interest*, BMC Public Health, **11** (2011), S4.

[41] L. Simonsen, T. A. Reichert, C. Viboud, W. C. Blackwelder, R. J. Taylor and M. A. Miller, *Impact of influenza vaccination on seasonal mortality in the US elderly population*, Arch. Intern. Med., **165** (2005), 265–272.

[42] J. M. Tchuenche, S. A. Khamis, F. B. Agusto and S. C. Mpeshe, *Optimal control and sensitivity analysis of an influenza model with treatment and vaccination*, Acta Biotheor, **59** (2011), 1–28.

[43] W. W. Thompson, D. K. Shay, E. Weintraub, L. Brammer, C. B. Bridges, N. J. Cox and K. Fukuda, *Influenza-associated hospitalizations in the United States*, JAMA, **292** (2004), 1333–1340.

[44] W. W. Thompson, D. K. Shay, E. Weintraub, L. Brammer, N. Cox, L. J. Anderson and K. Fukuda, *Mortality associated with influenza and respiratory syncytial virus in the United States*, JAMA, **289** (2003), 179–186.

[45] S. Towers and Z. Feng, *Social contact patterns and control strategies for influenza in the elderly*, Math. Biosci., **240** (2012), 241–249.

[46] J. Truscott, C. Fraser, S. Cauchemez, A. Meeyai, W. Hinsley, C. A. Donnelly, A. Ghani and N. Ferguson, *Essential epidemiological mechanisms underpinning the transmission dynamics of seasonal influenza*, J. R. Soc. Interface, **9** (2012), 304–312.

[47] A. R. Tuite, D. N. Fisman, J. C. Kwong and A. L. Greer, *Optimal pandemic influenza vaccine allocation strategies for the Canadian population*, PLoS One, **5** (2010), e10520.

[48] P. van den Driessche and J. Watmough, *Reproduction numbers and sub-threshold endemic equilibria for compartmental models of disease transmission*, Math. Biosci., **180** (2002), 29–48.

[49] J. Wallinga and P. Teunis, *Different epidemic curves for severe acute respiratory syndrome reveal similar impacts of control measures*, Am. J. Epidemiol., **160** (2004), 509–516.

[50] J. Wallinga, P. Teunis and M. Kretzschmar, *Using data on social contacts to estimate age-specific transmission parameters for respiratory-spread infectious agents*, Am. J. Epidemiol., **164** (2006), 936–944.

[51] D. Weycker, J. Edelsberg, M. E. Halloran, I. M. Longini, Jr., A. Nizam, V. Ciuryla and G. Oster, *Population-wide benefits of routine vaccination of children against influenza*, Vaccine, **23** (2005), 1284–1293.

[52] J. T. Wu and B. J. Cowling, *The use of mathematical models to inform influenza pandemic preparedness and response*, Exp. Biol. Med. (Maywood), **236** (2011), 955–961.

[53] P. Zhang and P. M. Atkinson, *Modelling the effect of urbanization on the transmission of an infectious disease*, Math. Biosci., **211** (2008), 166–185.

[54] U.S. Census Bureau, International Data Base. Available from: `http://www.census.gov/population/international/data/idb/region.php`.

[55] Centers For Disease Control and Prevention, *Large-scale vaccination clinic output and staffing estimates: An example*, (2009). Available from: `www.cdc.gov/h1n1flu/vaccination/pdf/A-Wortley-H1N1-sample-clinic.pdf`.

[56] Centers For Disease Control and Prevention, *Use of influenza A (H1N1) 2009 monovalent vaccine. Recommendations of the Advisory Committee on Immunization Practices (ACIP), 2009*, MMWR Recomm. Rep., **58(RR-10)** (2009), 1–8.

[57] Centers For Disease Control and Prevention, *Preventing emerging infectious diseases: A strategy for the 21st century. Overview of the updated CDC plan*, MMWR Recomm. Rep., **47(RR-15)** (1998), 1–14.

Received October 31, 2012; Accepted March 17, 2013.

E-mail address: eunha-shim@utulsa.edu